Astronomical and Astrophysical Transactions (*AApTr*), 2010/2011, Vol. 27, Issue 1, pp. 51–59,
ISSN 1055-6796, Photocopying permitted by license only, ©Cambridge Scientific Publishers

The double-peaked galaxy 3C390.3. II. An additional BLR associated with the jet?

L.S. NAZAROVA[1*] AND N.G. BOCHKAREV[2†]

[1]*Euro-Asian Astronomical Society, Universitetskij Pr. 13, Moscow, 119899, Russia;*
[2]*Sternberg Astronomical Institute, Universitetskij Pr. 13, Moscow, 119899, Russia*

Received 19 November, 2008

Analysis of UV and optical spectra of the radio galaxy 3C 390.3 shows that the observed line ratios for the broad components of lines CIV/Lα, Lα/Hβ and Hα/β can be best explained by two systems of clouds (two components to the BLR). One BLR component has an electron density 10^{10-12} cm^{-3} and is located in the equatorial plane at the distance ≈20 days from the center. This disk-like region emits predominantly low-ionization lines (including Hβ and Hα). The second BLR corresponds to the region with somewhat lower (10^{8-9} cm $^{-3}$), located out of the equatorial plane in the direction of radio-jet. Gas in this region could extend out to a distance of ≈ 40–80 days from the center. This region emits the high-ionization CIV line, a significant part (≈60%) of Lα and far wings of the Balmer lines.

Keywords: Galaxies: active; Galaxies: nuclei; Galaxies: individual (3C390.3); Galaxies: Seyfert, Double-peaked emission lines; Modeling: Broad line region

1 Introduction

The double-peaked galaxy 3C 390.3 is the prototype of the class of AGNs showing complex broad-line profiles with displaced distributions and/or an anisotropic illumination of the broad-line region (BLR). The double-peaked emission lines are often used as a strong indication of disk presence [1, 2]. The outflowing biconical gas stream [3] and binary black holes [4, 5] were also considered as a mechanism producing the double-peaked structure of the emission line.

However, the double peaked profiles in optical lines differ from single peaked UV line profiles in some galaxies. The different shape of the optical and UV lines indicates the existence of two line-emitting regions [6–8].

The time lag for optic and UV lines in 3C390.3 differs from other AGNs. The time lag for Hβ obtained from ground-based monitoring during 1994–1995 was 20±8 days [9] and initially it appeared that this was greater than the time lags of lines arising in the high-ionization region. According to the UV study, the lags for CIV line and Lα line are equal to 37±14 and 60±24 days respectively [10]. However, the study of

*Email: boch@sai.msu.ru
†Email: lsnazarova@rambler.ru

the optical spectra of 3C390.3 for period 1992–2000 [11] found the lag between the continuum and Hβ emission line variations to be 89±11 days and the lag of the Hα line was found to be 162±32. This differs from a previous study [9], which is probably due to sampling effects. Top maximal (flat-top peaks near $\approx 30^d$ and $\approx 100^d$) on the cross-correlation function (CCF) for Hβ broad component variation delay in respect to the optical continuum based on 3C390.3 monitoring during 1996–2001 have been found in [12].

The discovery of the correlation between the variations in the optical continuum and the variations from the radio-jet [13] indicates that UV and optic lines may also emit from the regions close to the radio-jet. We plan to consider this possibility and estimate the contribution to the emission in the lines from the regions located in the disk and around the jet.

The paper is organized as follows. The information about the observational data are presented in Section 2. The results of the analysis of the line profiles are given in Section 3. We discuss the results of the line ratios modeling in Section 4.

2 Observational data

The UV and optical spectra of 3C390.3 were taken from the AGN Watch database for the period January 1995 – January 1996. We took the UV and optic spectra at times of maximum and minimum luminosity during the taken period. The optic spectra were chosen from the files where Hα and Hβ are presented at the same file. It differs slightly from our first paper about 3C 390.3 [8]. Table 1 presents the information obtained from the AGN Watch database.

3 Analysis of the line profiles

The profiles of the CIV, Lα, Hβ and Hα lines have been divided into seven parts, the width of each part being equal to 2000 km s^{-1}. The core of the lines is measured between –1000 and +1000 km s^{-1}. Thus the blue and red wings have a width of ±7000 km s^{-1}. The difference of the line fluxes along of line profiles taken for Lα, CIV, Hβ and Hα lines show two clear components, one shortward which is better seen in UV lines and one near to the line center.

Figure 1 shows the CIV/Lα and Lyα/Hβ and Hα/Hβ line ratios as a function of velocity for the minimum and maximum states of the nuclear activity. The CIV/Lα ratio is low in the low-velocity regions of the line profile, but becomes higher in the blue wing, particularly when 3C 390.3 is more active. The asymmetry in the line ratios between the blue and red wings could be real, since the blue peak was stronger at this time, but it could also be an artifact of the extreme difficulty in removing NVλ1240 emission from the wing of Lα in an object with line profiles as complex as 3C 390.3.

The observed Lα/Hβ ratio is high at low velocity and decreases in the wings for both high and low states of the nuclear activity. This velocity dependence is the opposite of what is seen for most AGNs [7], where Lα is usually broader than the

Table 1 Data on line and continuum fluxes.

Line	Max	Min	Mean Flux	Var	Var/Mean%
Lα	15.42	9.48	12.45	5.94	47.7
CIV	14.35	5.82	10.08	8.53	84.6
Hβ	2.6	1.8	2.2	0.8	36.3
Hα	12.70	9.43	11.06	3.27	29.5
F_ν(1370A)	12.9	3.3	8.1	9.6	118.5
F_ν(5177A)	2.7	1.29	3.99	1.41	35.3
CIV/Lα	0.93	0.61	0.77	1.44	183.1
Lα/Hβ	5.93	5.26	5.65	7.42	131.3
Hα/Hβ	4.88	5.23	5.03	4.09	81.3

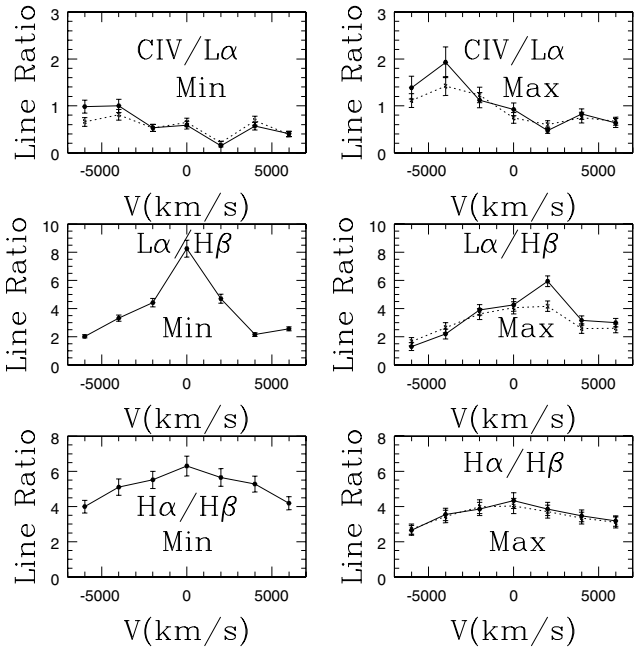


Figure 1 Line ratios CIV/Lα, Lα/Hβ and Hα/Hβ for the minimum (left side) and for maximum (right side) states of nuclear activity of 3C 390.3. The line ratios are shown for two periods: 1) close to the minimum – JD244733, 244785 in the hydrogen lines and 2449741, 2449782 in UV line; 2) close to the maximum – JD2450049,2450068 in the hydrogen and UV lines.

Balmer lines. This ratio strongly depends on the reddening effects. However taking into account this effect can increase Lα/Hβ ratio along the line profiles but cannot change the width of lines. The Hα/Hβ ratio is higher at low velocity in both the minimum and the maximum of nuclear activity. This ratio also depends on reddening effects and after taking into account this effect the Hα/Hβ ratio should decrease along the line profiles.

4 Photoionization models

The broad line spectrum is computed with so-called "photoionization models". Most popular at present is the photoionization cod "CLOUDY" which consist of a shell of gas (or cloud) in ionization and thermal equilibrium under the action of an external flux of radiation illuminating one face. We have used CLOUDY v. c90.05 [14] in its plane parallel version and assuming solar abundances. Photoionization models rely on the following input parameters: the flux and gas density, the spectral distribution in incident continuum, the column density and the element abundances. Since the element abundances have been assumed solar we shall discuss other input parameters.

4.1 Flux density

The flux density νF_ν was taken in our calculations as surface flux density at the illuminated face of the cloud (erg cm^{-2} s^{-1}) at frequency. 0.1 Ryd. The observed fluxes in 3C390.3 for the period January 1995 – January 1996 at maximum and at minimum nuclear activity taken at 1370 A [10] equals $12.7 \cdot 10^{-15}$ erg cm^{-2} s^{-1} A$_{-1}$ and $3.3 \cdot 10^{-15}$ erg cm^{-2} s^{-1} respectively.

Keeping in mind that the time lag for the Hβ line could be ≈80 days [11, 12], or perhaps as short as ≈20 days [9], we considered two different regions located at a different distance from the center. Hβ is emitted mainly from the Low Ionization Line region (LIL) which is commonly believed to be located in a disk, but the CIV and Lα lines are from the High Ionization Line region (HIL) which is probably located above an accretion disk [15–17]. Given the high velocity of the disk-like emission in 3C 390.3, it seems possible that emission from the LIL zone could produce a small lag for the Hβ line (e.g., ≈ 20 days) while the HIL region, which emits the significant part of the high-ionization lines (such as CIV and Lα with lags ≈ 40 and ≈ 60 days respectively), may be responsible for the large lag for the Hβ line ($\leq$ 80 days).

Thus, the flux density in calculations have been taken for distances from the nucleus 20, 40, 60 and 80 day for both maximum and minimum state of nucleus activity.

4.2 Gas density

The main difference in conditions between the different emission-line regions must be in density. To compare the observed line ratios with the models, we assumed, for simplicity, that the lines were produced from *the same* gas clouds (i.e., a single component) and investigated how conditions vary with velocity. Since the relative contributions from the different regions change with velocity, we can infer differences in density in the two regions. We calculated models covering a range of electron density from 10^7 cm^{-3} to 10^{13} cm^{-3}.

4.3 Spectral distribution

The assumed spectral distribution of the central continuum taken from [18].

4.4 Column density

The geometrical thickness, h, is assumed to be not larger than 10 light days. It means that when the density is large (typically $\geq 10^9$ cm^{-3}), we can follow the computation until the temperature falls below 4000 K, where there is no more optical emission. When the density is small, we stopped the computation at a column density (N_h) such that Log (N_h) = 25 cm^{-2} because, for the electron densities $\leq 10^9$ cm^{-3}, the column density is then small, favoring the emission of both the high- and low-velocity emission of broad-line regions arises from predominantly optically-thick clouds.

4.5 Calculations

The computed line ratios of CIV/Lα, Lα/Hβ and Hα/Hβ for a given central luminosity at the minimum and the maximum of 3C390.3 are shown in Fig. 2. Comparison of the observed (Fig. 1) and computed (Fig. 2) C IV/Lα, Lα/Hβ and Hα/Hβ line ratios could give information about the variety of the electron density along the line profiles. The observed line ratios: C IV/Lα, Lα/Hβ and Hα/Hβ show that the ratios

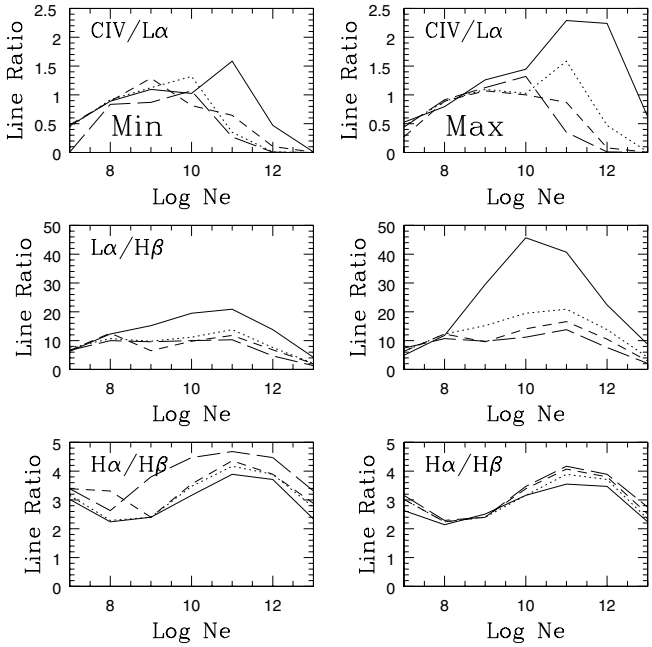


Figure 2 C IV/Lα, Lα/Hβ and Hα/Hβ line ratios versus electron densities. The calculated line ratios at distances from the center: 20 (solid line), 40 (dotted line), 60 (short-dash line) and 80 (long-dash line) days for the minimum and the maximum of nucleus activity.

varies along the line profiles. The ratio C IV/Lyα ratio varies across the line profile (0.2–0.8 at minimum to 0.4–1.5 at maximum). According to the UV study the lag of CIV and Lα are equal to 37±14. and 60±24 days respectively [10]. Therefore, the theoretical line ratios (dotted and short-dashed lines in Fig. 2) could be explained as:

a) the electron density 10^{7-8} cm^{-3} in the center of lines and increasing to the density 10^{10-11} cm^{-3} in the wings for the distance 40–60 days;

b) the electron density 10^{10-11} cm^{-3} in the wings increasing to 10^{12-13} cm^{-3} at the line center.

The center of lines has a contribution from low-density gas of NLR which was not removed because of the poor wavelength resolution of the IUE satellite's observations. Besides that the change in the CIV/Lα ratio with the changing continuum level also argues for the density increasing from $\sim 10^7$ cm^{-3} in the core to $\sim 10^{10}$ cm^{-3} in the wings, because the change in the ratio with luminosity is slight, as is predicted by Fig. 2. This would not be the case were the density $\sim 10^{12}$ cm^{-3} because there would be a stronger change in the CIV/Lα ratio.

Figure 1 shows that in both high and low states the Lyα/Hβ and Hα/Hβ ratios is highest at low velocities and decreases at higher velocities.

Although we do not correct for reddening CIV/Lα ratio which is not expected to be significant (inside the error-bar) the Lα/Hβ and Hα/Hβ ratios, however, *is*??? are strongly reddening dependent, and this must be taken into account in our analysis. For a radio-loud FR II AGN like 3C 390.3, Gaskell and coworkers [19] find a typical reddening, E(B-V) of the order of 0.3–0.7 mag. or so. Using the flat nuclear reddening curve they find for radio-loud AGNs like 3C 390.3 (see their Appendix 1), this implies that the Lα/Hβ ratios in Fig. 1 must be multiplied by a factor of $\sim$2 to $\sim$4. If we accept that reddening correction by factor 2 it gives the changes in Lα/Hβ could be 4–16 at minimum and 4–8 at maximum. The Lα/Hβ ratio is high in the center and decrease in the wings It corresponds:

a) to the density from 10^{10-12} cm^{-3} at the line center and increasing to the density to 10^{13} cm^{-3} or more at the line wings for the distance $\approx$ 40–80 days from the center;
or

b) to the density 10^{10-12} cm^{-3} at the line center and the density 10^{7-9} cm^{-3} at the wings for the distance from the center 40–80 days.

The observed low line ratio Hα/Hβ (4–6) at minimum and (3–4.5) at maximum will be decreased for both states to $\approx$(2–4) accepting the same reddening correction. Then the theoretical line ratio Hα/Hβ cannot be predicted to be less than 2 in the wings even for distance from the center 20 days (solid line) and could corespond to 10^{10-12} at the center and to 10^{13} or more at the wings. However the time lag for the Hβ line could be also $\approx$80 days [11, 12]. Without correction for reddening (which might be not significant at the distance of 80 days from the center if it is localized above an accretion disk) this corresponds to the theoretical line ratio Hα/Hβ 10^{10-12} cm^{-3} at the line wings and decreasing to 10^{8-9} cm^{-3} at the wings of the lines (long-dashed line).

The theoretical line ratio Hα/Hβ which is high in the center and low in the wings could correspond:

a) to 10^{10-12} cm^{-3} in the center of lines but increasing to 10^{13} cm^{-3} or more in the wings at the distance 20–80 days from the center:
or

b) to 10^{10-12} cm^{-3} in the line center but decreasing to 10^{8-9} cm^{-3} in the wings at the distance 20–80 days.

Thus, all these results support the suggestion that there are two different emission

regions with different densities:

- a low-density region with density: 10^{8-9} cm^{-3} located at the distance 40–80 days from the center;

- a high-density gas with the density 10^{10-12} cm^{-3} or more located at the distances 20–80 days.

Let us consider the case where the electron density obtained from the ratio of the high ionization lines CIV/Lα and from regions emitted in low ionization lines Hα and Hβ and located at the distance about 40–80 days from the center corresponds to the HIL zone. The electron density in the HIL zone decreasing from the wings to the center of these lines: $n_e \approx 10^{8-9}$ cm^{-3}. While the LIL zone has a higher electron density: N$_e$≈10^{12-13} cm^{-3} or more.

It is interesting to notice that the observed variable line ratios: CIV/Lα = 1.44, Lα/Hβ = 7.42 and Hα/Hβ = 4.09 (Table 1). The theoretical electron density for the observed variable line ratios without the reddening correction) is approximately 10^{9-10} cm^{-3} but for distances 40–80 days from the center which show that the most variable part of emission lines possibly emit from the low-density region and from the region with low reddening correction.

4.6 Contribution from zones

The contribution from the LIL zone with high electron density N$_e$≈10^{10-12} cm^{-3} should be significant in order to predict the observed low line ratio Lα/Hβ although the contribution to the emission in Lα from LIL zone cannot predict the observed CIV/Lα line ratio. Let us accept that summary emission in the line comes from both regions LIL and HIL and equals 100%: (LIL + HIL) = 100%. Then emission in the line comes from HIL region, HIL% = (100 - LIL)%. Figure 3 presents the CIV/Lα, Lα/Hβ and Hα/Hβ line ratios versus the contributions from LIL and HIL regions. The dash line shows the line ratios presented in Fig. 1.

Figure 3 shows that 40–60% contribution from the HIL region could predict the observed variable line ratio (Table 1) Lα/H$\beta \approx$ 7.42 if the regions located at the distances from the center of 40–80 days. However the low line ratio at the wings Lα/H$\beta \approx$ 2 could be predicted in LIL region only. The emission in the observed wings of CIV/L$\alpha \approx$ 1 and at the center of Hα/H$\beta \approx$ 4 line ratios can be explained by the emission only from the HIL and LIL regions respectably. However the variable part of Hα/H$\beta \approx$ 2 could be due to the emission from m HIL zone located at distances ≈ 80 days. The wings of CIV/Lα line ratio emits mainly from the HIL zone located at the distances ≈ 40–80 days but the center of that ratio which is low may have a weak contribution from the LIL zone. The contribution from the LIL zone to the emission in the center of CIV/Lα line ratio should be not significant since the emission in the line CIV is reducing dramatically with the electron density more than 10^{11} cm^{-3} and at distances from the center corresponding more than 40 days.

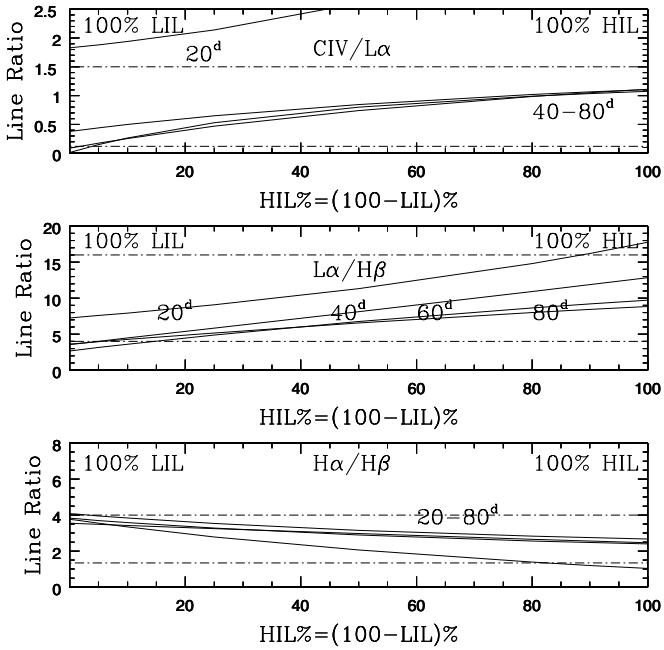


Figure 3 The relative contribution from BLR and NLR to the calculated emission lines.

5 Discussion

The double peaked Hα profile is a strong argument for a Keplerian disk model the emission lines. However, the careful analysis variability amplitudes, profile changes and profile evolution in Broad Balmer lines [11] are pointed out on some problems. They found a few arguments against the disk interpretation. 1) The high-velocities components which according to a disk model should arise in the inner part of the disk and therefore be most responsible to continuum variations. Nevertheless the high-velocities features show a poor correlation between continuum and far profile wings. 2) There are strong differences in the behavior of the very near wings (central red and blue parts show that the broad line profiles cannot be entirely attributed to a disk. 3) Observed evolution of the Balmer line profiles shows that the profile changes are clearly not reverberation effects. Thus, Sergeev and coworkers [11] came to the conclusion that there may be an additional profile component with different behavior of the near wings of the lines. Similar suggestion from the analysis of the physical conditions along the line profiles discussed in [8].

The discovery of the correlation between the variations in the optical continuum and the variations of the radio flux from the radio-jet [13] show that the BLR might exist not only at the disk but also near to the radio-jet. According to our calculations and to the lags for Balmer and UV lines obtained by AGN Watch campaign seems to suggest that the model with two BLRs which have a different locations may solve the problems.

The BLR1 is traditionally located at the disk at a distance of, according to the hydrogen lines, ≈20 days. This disk-like region emits predominantly low ionization lines located in the equatorial plane where the BLR covering approaches 100% similar to BLR in NGC5548 [20]. The BLR2 forms around the radio-jet and is located at a distance of ≈ 40–80 days from the center. The BLR2 responsible for the emission in the UV lines (CIV line is varied at 84%, according to Table 1). The Lα line partly forms in BLR2 – 40–60% and partly in BLR1. The bulk of the hydrogen lines forms at the disk and the wings – near to the radio-jet at the distance from the center ≥80 days.

That model may also explain the observed Lα/Hβ line ratio which is high at the center of lines and low in the wings. That contradicts other galaxies similar to NGC 5548 [7], where the low ratio of Lα/Hβ lines is observed at the line center. This pointed out that there is a significant contribution to the disk emission from an additional source – emission from the region near the radio-jet.

Acknowledgements

We acknowledge the support under the RFBR Grant 09-02-01136.

References

[1] K. Chen and J.P. Halpern, (1989) ApJ, 344,115.
[2] Eracleous, M. and Halpern, J.P. (1994) ApJS, 90, 1.
[3] Veilleux, S. and Zheng, W. (1991) ApJ, 377, 89.
[4] Peterson, B.M., Korista, K.T. and Cota, S.A. (1987) ApJ 312.
[5] Gaskell, C.M. (1996) ApJ, L107.
[6] Eracleous, M., Halpern, J.P. and Charlton, J.C. (2003) ApJ, 582, 633.
[7] Snedden, S.A. and Gaskell, C.M. (2004) ASPC, 311, 197S.
[8] Nazarova, L.S., Gaskell, C.M., Klimek, E. and Bochkarev, N.G. (2004) AAT 23, 343.
[9] Dietrich, M. *et al.* (1998) ApJS, 115, 185D.
[10] O'Brien, P.T. *et al.* (1998) ApJ, 509, 1630.
[11] Sergeev, S.G. *et al.* (2002) ApJ 576, 660.
[12] Shapovalova, A.I. *et al.* (2002) ASSL, 274, 279V.
[13] Arshakian, T.G., Leon-Tavares, J., Lobanov, A.P., Chavushyan, V.H., Shapovalova, A.I., Burenkov, A.N., and Zensus, J.A. (2010) MNRAS 401, 1231A.
[14] Ferland, G.J., Korista, K.T., Verner, D.A., Ferguson, J.W., Kingdon, J.B. and Verner, E.M. (1998) PASP, 110, 761.
[15] Collin-Souffrin, S. (1986) A&A, 166, 115.
[16] Gaskell, C.M. (2000) New Ast. Rev., 44, 563.
[17] Collin-Souffrin, S. and Lasota, J.-P. (1988) PASP, 100, 1041.
[18] Grandi, P., *et al.* (1999) A&A, 343, 33.
[19] Gaskell, C.M., Grossmann, R.W., Antonucci, R.R.J. and Whysong, D. (2004) ASPC, 311,61G.
[20] Gaskell, C.M., Klimek, E.S. and Nazarova, L.S. (2007) arXiv 0711, 1025G.